Tan *et al. EURASIP Journal on Wireless Communications and Networking* (2018) 2018:210
https://doi.org/10.1186/s13638-018-1223-1

EURASIP Journal on Wireless Communications and Networking

RESEARCH Open Access

Multiuser precoding scheme and achievable rate analysis for massive MIMO system

Weiqiang Tan[1], Wei Huang[2], Xi Yang[3], Zheng Shi[4], Wen Liu[2] and Lisheng Fan[1*]

Abstract

We analyze the downlink multiuser precoding of massive multiple input multiple output (MIMO) system, where the base station (BS) has ideal channel state information (CSI) and adopts three types of different linear precoding schemes, i.e., maximum ratio transmission (MRT), zero-forcing (ZF), and minimum mean squared error (MMSE). Under a Rayleigh fading channel, we attain the exact expressions on the achievable rate for these three precoding schemes. Moreover, we provide several insights on the achievable rates and reveal the relation of the number of BS antennas, the number of users, and the input signal-to-noise ratio (SNR) with the achievable rates respectively. It is found in general that the achievable rate increases with the number of BS antennas and the input SNR. To be more specific, the MRT precoding scheme is much inferior to the ZF and MMSE precoding schemes and tends to be at a fixed rate at the high SNR case. On the contrary, the MRT precoding scheme outperforms ZF precoding schemes at the low SNR case. Moreover, the total achievable rate always does not increase with the number of users and the optimal number of users always exists for the ZF and MMSE precoding schemes.

Keywords: Achievable rate, Multiuser massive MIMO, Linear precoding scheme, Maximum ration transmission, Zero forcing, Minimum mean square error

1 Introduction

Massive multiple input multiple output (MIMO), well viewed as one of the important techniques for fifth generation (5G) wireless communication, has attracted a great deal of research interest in current years [1–3]. The main idea of massive MIMO is to deploy a large-scale number of antennas and employ some simple precoding processing or detection technologies at the base station (BS), which significantly reduces the impact of noise and user interference, and hence, spectral efficiency (SE), energy efficiency, transmission reliability, and quality of service (QoS) can be significantly improved [4–7]. However, with the greatly increasing number of BS antennas, maybe up to dozens or even hundreds, the design of massive MIMO system brings up the new challenges. Therefore, various potential techniques for massive MIMO system must be well specified before its roll-out [8–11].

*Correspondence: lsfan@gzhu.edu.cn
[1]School of Computer Science and Educational Software, Guangzhou University, 510006 Guangzhou, People's Republic of China
Full list of author information is available at the end of the article

1.1 Related work

So far, several aspects of massive MU-MIMO system, including channel measure, channel estimations, pilot contamination, and precoding schemes, have been investigated. For example, the authors in [12] measured real massive MIMO channel model, in which the BS is deployed a cylindrical antenna array configuration. Measurements showed that channel vectors between the different users were not actually pairwise orthogonal when the BS is deployed the finite number of antenna elements. The work in [13, 14] considered a uniform cylindrical array configuration equipping with hundreds of antenna elements. Measurement results showcased that compared with conventional MIMO systems, the MIMO channel model show greater correlation and without wide sense stationary properties. A similar investigation was conducted in [15]. Moreover, when the number of antennas become very large, the availability of perfect CSI gets very tricky, which also becomes another important issue in massive MIMO systems [16]. By exploiting user preference and spatial locality, the authors in [17, 18]

investigated the optimal cache policy to minimize the average file download time in massive MIMO system. The work in [19] proposed the coordinated channel estimation for massive MIMO system by exploiting the second-order statistical information. In multi-cell massive system, the channel estimation at the target cell is contaminated by non-orthogonal pilot sequences by users in adjacent cells, the pilot contamination becomes a severe bottleneck. To effectively suppress the pilot contamination, a time-shifted scheme was proposed in [20], which aims to resolve the effects of pilot contamination. The work in [21, 22] proposed a pilot sequence coordination scheme; the pilot combinations are efficiently eliminated by sharing the different pilot sequence among each cells.

In massive multiuser MIMO systems, some linear precoding scheme is of great importance since it is very popular in practical applications and enables to significantly improve the performance. The work in [23, 24] studied the performance of massive MIMO systems that contain the achievable SE and energy efficiency, respectively, where the BS adopts only MRT precoding and knows the accurate CSI. An accurate theoretical result for the achievable rate is derived firstly. Then, considering a realistic energy consumption model [25, 26], the expression of energy efficiency is also obtained. Results showed that the massive antennas equipped in the BS can do boost system performance. Most of the research about massive MIMO systems mainly concentrates upon the theoretical studies and usually assume that the massive MIMO system experiences the i.i.d. Rayleigh fading channels. In [27], the uplink achievable rates with perfect or partial CSI were derived. Scaling laws were applied in terms of the power savings in massive MIMO systems as the number of BS antennas increased. With an arbitrary-rank deterministic component, expressions under perfect or imperfect CSI for uplink achievable rates were derived in [28]. Moreover, for the downlink transmission, authors in [29] investigated the achievable sum-rate of downlink massive MIMO systems with MRT and ZF precoders, but they did not give the exact expression. In addition, the total achievable rate was investigated of massive MIMO systems, where the MRT and ZF precoding schemes ware performed in [30], some simplified closed-form formulas for the achievable rate were derived in the high and low signal-to-noise ratios (SNR) regimes. From the prior work review, it can be found that there is no work to establish a comprehensive analysis on the achievable rate for MRT, ZF, and MMSE precoding schemes, especially for the exact expression on the achievable rate that remains a longstanding challenge in massive MIMO system.

1.2 Contributions

In order to compensate for this gap, this paper provides a deep investigation of centrical massive MIMO systems and adopts three different linear precoding. Our main contributions are as follows:

- We consider a general Rayleigh fading channel model[1] and obtain the exact expressions on the achievable SE of massive MIMO systems for MRT, ZF, and MMSE precoding schemes by exploiting the theory of large dimensional random matrix and the probability density function (p.d.f.) of random variables.
- According to the derived exact expressions, we explore the tractable approximated expressions on the achievable rate. Additionally, based on the derived theoretical results, we further illustrate how the achievable rate changes as the number of BS antennas and number of users, as well as the input SNR on the total achievable rate.
- Our results indicate that the achievable rate increases with the number of BS antennas and the input SNR for different linear precoding and there exists the best number of users for ZF and MMSE precoding scheme. In addition, the achievable rate shows that the ZF and MMSE precoding schemes achieves higher achievable rate than MRT precoding schemes at the high SNR case. On the contrary, the precoding MRT scheme outperforms the precoding ZF and MMSE schemes at the low SNR case.

1.3 Methods or experimental

The rest of the paper is organized as follows. Section 2 presents the signal model and studies the achievable ergodic rate of massive MIMO system. In Section 3, by employing the theory of large dimensional random matrix and the p.d.f. of random variables, we derive analytical expressions of the achievable ergodic rate for MRT, ZF, and MMSE precoding techniques. According to the derived theoretical results, we attain the several engineering insights by considering the special cases. Section 4 provides the Monte-Carlo numerical simulation to confirm the obtained analytical results. Section 5 outlines the whole paper. Additionally, all the main proofs are given in the appendices.

Notations: Vector and matrix accounts for lower- and uppercase boldface, $(\cdot)^H$ and $[\cdot]_{kk}$ denote conjugate transpose and the kth diagonal element of the matrix, respectively, $\lfloor\cdot\rfloor$ and $\mathbb{E}\{\cdot\}$ represent rounding to the nearest integer and expectation operator, respectively, and $\mathbf{I}_N$ denotes the N dimensional identical matrix, $\mathbb{C}$ is a complex Gaussian, and γ represents the Euler-Mascheroni constant.

2 Signal model

In this section, we describe a downlink transmission signal model and introduce the MRT, ZF, and MMSE precoding

schemes. By utilizing different linear precoding schemes, we present the achievable ergodic rate of the centralized massive MIMO system.

2.1 Channel model

Consider the centralized massive MIMO system as exhibited in Fig. 1, in which the BS is deployed N_t transmitter antennas and there are Kusers being randomly distributed in the circular-shape cell. In this scenario, the $N_t$transmitter serves to Ksingle-antenna users at the same time frequency resources and we consider that the number of antennas is far greater than the number of users satisfying the limited condition $K \ll N_t$. Before all users received the transmitted date, the BS shall use some simple linear precoding techniques pre-process, which realizes the signal term maximization and interfere term minimization as much as possible. For the K users, the received vector is given by

$$\mathbf{y} = \sqrt{\rho}\mathbf{H}^H\mathbf{W}\mathbf{s} + \mathbf{n}, \tag{1}$$

where ρ accounts for the input SNR, $\mathbf{H} \in \mathbb{C}^{N_t \times K}$denotes channel matrix between N_t transmitter antenna and K users, $\mathbf{s}$ denotes a signal vector of $K \times 1$ dimensional, $\mathbf{n}$ represents the additive white Gaussian noise (AWGN), and $\mathbf{W}$accounts for a beamforming matrix, which enables to boosts the total achievable ergodic rate of massive multiuser MIMO system.

Though there exists many precoding schemes to improved the performance of the multiuser massive MIMO system, some precoding schemes are not easily implemented in the practical system, especially for the nonlinear precoding schemes, for example, vector perturbation (VP) and dirty paper coding (DPC), since they have much computation complexity. Considering the actual application requirements, we would like to study the general linear precoding scheme, which has been popularly used in the actual system. The beamforming matrix of the MRT, ZF, and MMSE precoding schemes is modeled as

$$\mathbf{W} = \begin{cases} \mathbf{H} & \text{for MRT} \\ \mathbf{H}\left(\mathbf{H}^H\mathbf{H}\right)^{-1} & \text{for ZF} \\ \mathbf{H}\left(\mathbf{H}^H\mathbf{H} + \frac{1}{\rho}\mathbf{I}_K\right)^{-1} & \text{for MMSE} \end{cases} \tag{2}$$

where $\mathbf{W}$ accounts for the precoding matrix that is determined by the precoding schemes. Herein, $\mathbf{W} = [\mathbf{w}_1, \mathbf{w}_2, \ldots, \mathbf{w}_K]$ that relies on the channel matrix of $\mathbf{H}$.

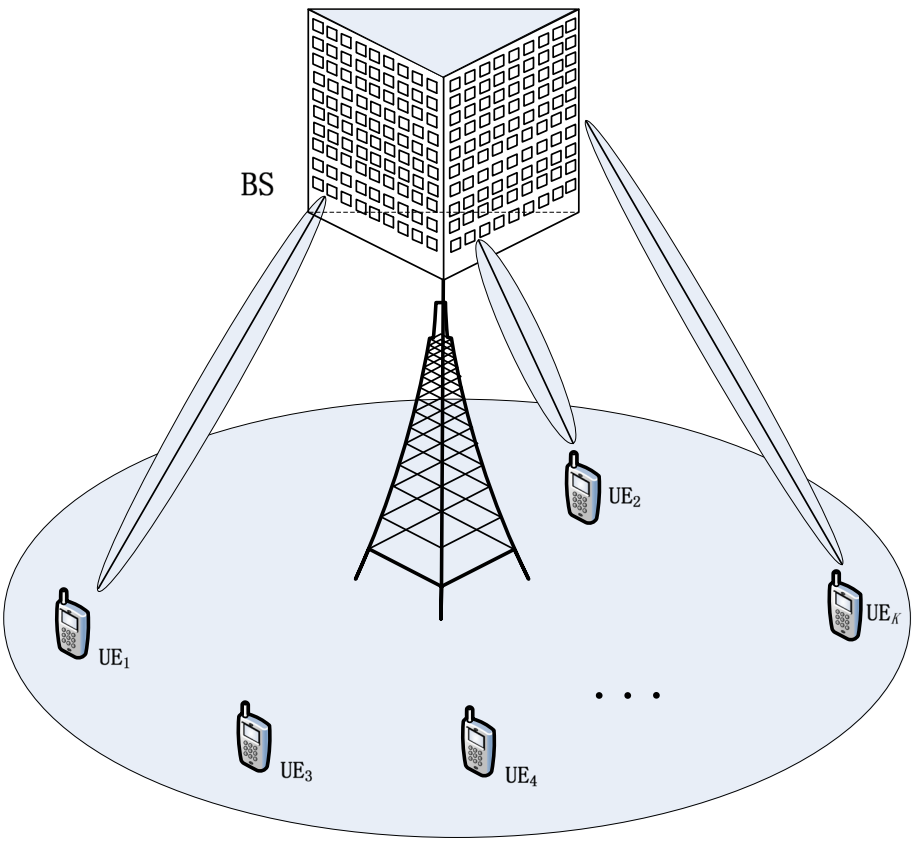

Fig. 1 A schematic diagram of a massive MU-MIMO system equipped with N_t transmit antennas serving K users

2.2 Achievable ergodic sum-rate analysis

We assume that the perfect and instantaneous channel state information (CSI) is available at the BS, which can potentially be obtained for massive MIMO system, such as in frequency division duplex (FDD) mode, where the BS acquires the perfect CSI through exploiting uplink channel feedback. In time division duplex (TDD) mode, the perfect CSI is acquired by the BS through open-loop uplink pilot training. Before the transmitter symbol, the BS adopts the three different linear precoding schemes. At the users terminal, each user receives a symbol via predecoding, thus the received signal at the user $k$is given by

$$y_k = \sqrt{\rho}\mathbf{h}_k^H \mathbf{w}_k s_k + \sqrt{\rho}\sum_{j=1, j\neq k}^{K} \mathbf{h}_k^H \mathbf{w}_j s_j + n_k, \tag{3}$$

where $\mathbf{h}_k \in \mathbb{C}^{N_t \times 1}$represents the kth column of the channel vector $\mathbf{H}$, whose entries are i.i.d. complex Gaussian random variable. Similarly, $\mathbf{w}_k$ denotes the kth column vector of precoding matrix $\mathbf{W}$ that satisfies limited condition $\|\mathbf{w}_k\| = 1, \forall K$, s_k and s_j represent transmit symbols for the user k and j, and n_k the addition Gaussian noise with zero mean and unit variance, which is widely used in the previous literature [31, 32]. According to the signal model in (3), we can write the achievable ergodic rate of the user k, which is calculated as[2]

$$R_k^* = \mathbb{E}\left\{\log_2\left(1 + \frac{\rho\left|\mathbf{h}_k^H \mathbf{w}_k\right|^2}{1 + \rho\sum_{j=1, j\neq k}^{K}\left|\mathbf{h}_k^H \mathbf{w}_j\right|^2}\right)\right\}. \tag{4}$$

From (4), it can be seen that the achievable ergodic rate is a logarithmic function of SINR. In order to maximize the SINR term, the most intuitive approach is to enhance the signal term in the numerator and suppress the interference term in the denominator. In the following, we shall adopt different precoding schemes to study the achievable ergodic rate of system.

3 Exact expression on the achievable rate

This section aims to obtain exact expressions on the achievable ergodic rate by considering different precoding schemes. Employing the obtained theoretical results, we attain the several interesting effect of physical insights on the achievable rate of the massive MIMO system.

3.1 Achievable rate analysis with MRT precoding

We first consider the MRT precoding scheme for the massive MIMO system due to it has considerably low computation complexity. The precoding matrix comes form the conjugate transpose of the channel matrix, which does not involve operations of matrix inverse. In three type linear precoding schemes, the MRT precoding scheme is simple and has low complexity, thus it is the most popular for massive MIMO systems.

To proceed, we first study the achievable ergodic rate when the BS adopts the MRT precoding scheme, and then we draw several insights into the system performance.

Theorem 1 *When the BS employs the MRT precoding scheme under the Rayleigh fading channel model, the exact expression on the achievable ergodic rate of the user kis calculated by*

$$R_k^{MRT} = \log_2(e)e^{\frac{1}{\rho}}\sum_{h=K}^{N_t+K-1} E_h\left(\frac{1}{\rho}\right), \tag{5}$$

where $E_h(\cdot)$denotes the exponential integral function of order h. For real non-zero values of x and the integer h, the exponential integral $E_h(x)$is defined as

$$E_h(x) = \int_1^{\infty}\frac{e^{-xt}}{t^h}dt. \tag{6}$$

Proof See Appendix 1. □

From *Theorem* 1, it can be seen that the achievable ergodic rate is associated with the number of BS antennas, the input SNR, and the number of users. Considering this sophisticated expression in (5) involves the exponential integral function, which makes the engineering insight become intractable. To gain more insights into the performance, we introduce the following tractable approximated expression on the achievable rate.

Corollary 1 *When the BS employs the MRT precoding scheme under the Rayleigh fading channel model, an approximated expression on the achievable SE can be given by*

$$\tilde{R}_k^{MRT} = \log_2\left(1 + \frac{\rho N_t}{1 + \rho(K-1)}\right). \tag{7}$$

Proof Before the proof, we factorize (5) into

$$R_k^{\mathrm{MRT}} = \log_2(e)e^{\frac{1}{\rho}}\left(\sum_{h=1}^{N_t+K-1} E_h\left(\frac{1}{\rho}\right) - \sum_{h=1}^{K-1} E_h\left(\frac{1}{\rho}\right)\right). \tag{8}$$

When the value of Ngrows without bounds and further employs the result in ([33], Eq. (5.1.19)), we derive the following approximated identical that holds

$$e^{\frac{1}{x}}\sum_{n=1}^{N-1} E_n\left(\frac{1}{x}\right) \approx \log\left(1 + x(N-1)\right) \tag{9}$$

Substituting (9) into (8) and applying the above equivalent, the special function is calculated as (10), which can be found the top of the next page.

$$e^{\frac{1}{\rho}}\sum_{h=1}^{N_t+K-1}E_h\left(\frac{1}{\rho}\right)-e^{\frac{1}{\rho}}\sum_{h=1}^{K-1}E_h\left(\frac{1}{\rho}\right)\approx\log\left(1+\rho(N_t-K+1)\right)-\log\left(1+\rho(K-1)\right). \tag{10}$$

By plugging (10) into (8) and doing some mathematical manipulations. We finish the proof. □

From *Corollary* 1, it can be seen that the achievable ergodic rate is a monotonically increasing logarithmic function of number of BS antennas. It implies that the larger number of antennas deployed at the BS, the bigger antenna diversity gain and multiplexing gain will be obtained. The observation implies that deploying a large-scale antenna at the BS plays an important role in massive MIMO systems and verifies the intuitive result in [34]. We consider the high-input SNR case and present the achievable ergodic rate limit in following corollary.

Corollary 2 *When the input SNR goes without bound, the achievable ergodic rate converges to the saturated rate that is calculated as*

$$\lim_{\rho\to\infty}\bar{R}_k^{MRT}=\log_2\left(1+\frac{N_t}{K-1}\right). \tag{11}$$

Proof The desired result can be derived by letting $\rho\to\infty$in (7). □

We can see that the result in (11) is highly independent of ρ and tends to a constant, whose value depends on the number of BS antennas and the number of users. Given the number of users, R_k^{MRT}increases with the number of BS antennas since it makes channel vectors being asymptotically orthogonal. On the other hand, with a fixed number of BS antennas, R_k^{MRT}decreases when the number of users increases indicating more degradation due to interference from more users. This is because that inter-user interference becomes significant. Next, we further study the achievable rate of massive MIMO system with ZF precoding scheme in the following section.

3.2 Achievable rate analysis with ZF precoding

Although the MRT precoding has a low computer complexity and is a powerful scheme in massive MU-MIMO systems, the achievable ergodic rate does always converge to fixed rate at the high SNR regime. Herein, we shall further study achievable rate of massive MIMO system with ZF precoding, because the ZF precoding scheme could completely eliminate interference among users, which achieves the performance rival that of the DPC scheme [35]. When ZF precoding scheme is adopted at the BS, the precoding matrix $\mathbf{W}$ can be written as [36, 37]

$$\mathbf{W}=\mathbf{H}^H\left(\mathbf{H}\mathbf{H}^H\right)^{-1}. \tag{12}$$

By using the ZF precoding scheme, the achievable ergodic rate of the user $k$is given by

$$R_k^{\mathrm{ZF}}=\mathbb{E}\left\{\log_2\left(1+\frac{\rho}{\left[\left(\mathbf{H}^H\mathbf{H}\right)^{-1}\right]_{kk}}\right)\right\}, \tag{13}$$

where the expectation is taken over all vector realizations of channel matrix $\mathbf{H}$ that is assumed to be ergodic.

Theorem 2 *When the BS employs the ZF precoding schemes under the Rayleigh fading channel model, the exact expression of the achievable ergodic rate is expressed as*

$$R_k^{ZF}=\log_2(e)e^{\frac{1}{\rho}}\sum_{h=1}^{N_t-K+1}E_h\left(\frac{1}{\rho}\right), \tag{14}$$

where the special function $E_h(\cdot)$is defined in (6).

Proof See Appendix 2. □

From *Theorem* 2, the achievable rate is significantly associated with the number of BS antennas, the number of users, and SNR. Furthermore, it is shown that the exact expression of (14) have remained elusive because it involves exponential integral functions and becomes more sophisticated and complicated. Therefore, it is hard to offer the intuitive physical insight. To handle these disadvantages, we try to derive tractable approximated expression that could let us have intuitive insights. These insights establish a compelling rationale for massive MIMO system. The following corollary derives an approximated expression on the achievable SE.

Corollary 3 *When the BS employs the ZF precoding under the Rayleigh fading channel model, an approximated expression on the achievable SE can be given by*

$$\bar{R}_k^{ZF}=\log_2\left(1+\rho\left(N_t-K+1\right)\right) \tag{15}$$

Proof Recalling that the approximated expression in (9), by applying the same method, we obtain

$$e^{\frac{1}{\rho}}\sum_{h=1}^{N_t-K+1}E_h\left(\frac{1}{\rho}\right)\approx\log\left(1+\rho(N_t-K+1)\right). \tag{16}$$

Substituting (16) into (14), we obtain the desired result. □

From *Corollary* 3, we can draw an interesting conclusion that R_k^{ZF} is significantly associated with the input SNR, the number of BS antennas, and the number of users. It is worthy to note that $\bar{R}_k^{\mathrm{ZF}}$ in (15) is a monotonically

increasing function with the number of BS antennas and the SNR. Additionally, it is noted that with fixed the number of BS antennas and SNR, $\bar{R}_k^{\mathrm{ZF}}$ in (15) is a monotonically decreasing function when the number of users increases due to average power designated for each user. However, as the number of users grows, the total achievable ergodic rate increases since it is the multiplication of the achievable ergodic per rate by the number of users. How does the total achievable ergodic rate change with the number of users and make the achievable sum-rate achieve maximum? Fixing the number of BS antennas and SNR, we shall reveal the changing trend of the total achievable ergodic rate in terms of the number of users.

Corollary 4 *When the BS employs the ZF precoding scheme under the Rayleigh fading channel model, a unique globally best number of users can be derived that achieves the total achievable rate maximization, the optimal number of users is expressed as*

$$K^{opt} = \left\lfloor \frac{\Delta}{\rho}\left(1 - \frac{1}{W_0(\Delta \exp(1))}\right) \right\rfloor. \tag{17}$$

where $\Delta = 1 + \rho\,(N_t + 1)$ *and* $W_0(\cdot)$ *represents the Lambert function that provided in* [38].

Proof We assume that the each user is randomly located and experiences the same distributed in the cell. Thus, the total achievable rate is equal to a sum of the K achievable rate, which is calculated as follow

$$\bar{R}_{\mathrm{sum}}^{\mathrm{ZF}} = K\log_2\left(1 + \rho\,(N_t - K + 1)\right). \tag{18}$$

From (18), it can be seen that as the number of users grows, the achievable ergodic rate per user decreases but the the achievable ergodic rate increases since it is the multiplication of the achievable ergodic per rate by the number of users. Therefore, we know that the function (18) is a convex problem with respect to the number of users and there exists a unique globally optimal number of users that achieves the total achievable rate maximization. We need to check the partial derivative respect to the number of users K, which will know its change varies with K clearly. We differentiate the total achievable rate in (18) in the terms of the number of users K, the first-order partial derivative of $R_{\mathrm{sum}}(K)$ can be calculated as

$$\frac{\partial \bar{R}_{sum}^{ZF}(K)}{\partial K} = \frac{1}{\ln 2}\left(\ln\left(1 + \rho(N_t - K + 1)\right) - \frac{\rho K}{1+\rho\,(N_t - K + 1)}\right). \tag{19}$$

From (19), we can see that the second term is equal to negative, it is hard to judge whether the values of (19) is strictly positive or negative. Therefore, we need to further check the second order partial derivative of $R_{\mathrm{sum}}(K)$ that holds

$$\frac{\partial \bar{R}_{\mathrm{sum}}^{\mathrm{ZF},2}(K)}{\partial K^2} = \left(\frac{-\rho K}{1 + \rho\,(N_t - K + 1)} + \frac{-\rho(N_t + \rho + 1)}{(1 + \rho\,(N_t - K + 1))^2}\right). \tag{20}$$

Then, it is inferred that $\partial \bar{R}_{\mathrm{sum}}^2(K)/\partial K^2 < 0$ due to the value of numerator is a negative, this shows that the function $R_{\mathrm{sum}}(M)$is concave with respect to M. According to convex optimization theory, we know that a unique globally optimal number of users always exists, which enables to achieve the total achievable SE maximization. To check the best value, set the first-order partial derivative to satisfy the following condition

$$K^{opt} = \left\{ K \middle| \frac{\partial \bar{R}_{\mathrm{sum}}^{\mathrm{ZF}}}{\partial K} = 0 \right\}, \tag{21}$$

Substituting (19) into (21), we have

$$\ln\left(1 + \rho\,(N_t - K + 1)\right) = \frac{\rho K}{1 + \rho\,(N_t - K + 1)}. \tag{22}$$

In order to solve the above equation in terms of random variable K, we observe that the equation is so sophisticated because it involves the logarithmic function. We use the associated analysis tool [39–41] and let $y = 1 + \rho\,(N_t - K + 1)$, (22) reduces to

$$(1 + \rho\,(N_t + 1))\exp(1) = \frac{1 + \rho\,(N_t + 1)}{y} \exp\left(\frac{1 + \rho\,(N_t + 1)}{y}\right). \tag{23}$$

According to the definition of the Lambert function [38], we can attain

$$y = \frac{1 + \rho\,(N_t + 1)}{W_0(1 + \rho\,(N_t + 1)\exp(1))}. \tag{24}$$

Substituting y into (24) and doing some mathematical manipulations. We finish the proof. □

From *Corollary* 4, it reveals an important result that if the achievable sum rate will not linearly increase with the number of users, it is a convex function. With the aid of the convex optimization theory, we know that there indeed exists the best number of users that achieves the total achievable rate maximization. Note that the value in (17) being an integer is not guaranteed, thus we need to make sure the optimal number of users are rounded to the nearest integer.

3.3 Achievable rate analysis with MMSE precoding

In this section, we consider the MMSE precoding schemes, which can be understood as the optical linear precoding schemes in massive MIMO system. The MMSE precoding is better than ZF precoding schemes, but it is

much complex than ZF precoding schemes, which can be achieved by the MMSE method.

When the MMSE precoding scheme is employed at the BS, the precoding matrix $\mathbf{W}$ can be given by [42]

$$\mathbf{W} = \mathbf{H}^H \left(\mathbf{H}\mathbf{H}^H + \frac{1}{\rho}\mathbf{I}_K \right)^{-1} \tag{25}$$

To facilitate the analysis, we derive the asymptotic SINR at the k-th user and rewrite the R_k^{MMSE}as follows

$$R_k^{\mathrm{MMSE}} = \mathbb{E}\left\{ \log_2 \left(1 + z_k\right) \right\}, \tag{26}$$

where

$$z_k = \frac{1}{\left[\left(\mathbf{H}\mathbf{H}^H + \rho \mathbf{I}_K \right)^{-1} \right]_{kk}} - 1. \tag{27}$$

Theorem 3 *When the BS employs the MMSE precoding scheme under the Rayleigh fading channel model, the exact expression on the achievable ergodic rate is expressed as*

$$R_k^{MMSE} = \log_2(e) e^{\frac{1}{\beta}} \sum_{h=1}^{\alpha} E_h \left(\frac{1}{\beta} \right), \tag{28}$$

where the parameter α is shown as

$$\alpha = \frac{\left(N_t - K + 1 + (K-1)\,\mu\right)^2}{N_t - K + 1 + (K-1)\,\theta} \tag{29}$$

and the parameter β is shown as

$$\beta = \frac{N_t - K + 1 + (K-1)\,\theta}{N_t - K + 1 + (K-1)\,\mu} \rho. \tag{30}$$

Additionally, the above parameters α and β is highly dependent on the following equations, whose values can be calculated by checking the following identical

$$\mu = \frac{1}{\rho\left(N_t - (K-1)\left(\mu - 1\right)\right) + 1} \tag{31}$$

and

$$\theta \left(1 + \frac{K-1}{\left(\rho\left(N_t - (K-1)\left(\mu-1\right)\right) + 1\right)^2} \right) = \frac{(K-1)\,\rho\mu + 1}{\left(\rho\left(N_t - (K-1)\left(\mu-1\right)\right) + 1\right)^2}. \tag{32}$$

Proof See Appendix 3. □

According to *Theorem* 3, we observe the exact expression on the achievable rate which involves several parameters and which is difficult for intuitive insight. This motivates us to present the numerical result to verify the analytical result in the following section.

4 Numerical results

In this section, we provide the numerical results by using the Monte-Carlo simulation, which aims to confirm the derived theoretical results that are provided in the above section. For fairness, we adopt the same configuration for massive MIMO system under different MRC, ZF, and MMSE precoding schemes. In all simulations, channel vectors are realized that come from the channel model in (3).

Figure 2 shows the achievable rate versus SNR for MRT, ZF, and MMSE precoding schemes, respectively. In our simulations, the number of users is set to $K = 10$, the number of BS antennas is $N_t = 128$ and the input SNR changes from -20 to 20 dB. As we can see that regardless of exact results or approximate results, the numerical curves greatly coincide with all theoretical curves, which confirms the theoretical analysis obtained in Section 3. Furthermore, we can see that at the low SNR case, the achievable rate with MRT precoding scheme is greater than the achievable rate with ZF precoding schemes, which implies that employing the MRT precoding scheme is a good choice when the transmit power is a limited condition. On the contrary, at the high SNR case, the achievable rate with ZF and MMSE precoding schemes achieves a higher achievable rate than that with MRT precoding schemes. As expected, the achievable rate with ZF and MMSE precoding schemes exponentially increases when the input SNR increases. This is because these schemes facilitate inter-user interference and noise cancelation. Moreover, the achievable rate with MMSE precoding schemes is always better than that with ZF precoding schemes, and the achievable rate with MRT scheme tends to have a fixed rate when the input SNR goes without bounds, which is a well predictor of the theoretical analysis in *Corollary* 2 due to the fact that the signal gain increases as the input SNR grows, while the inter-user interference also increases. Therefore, we will depict only the theoretical result when evaluating performance in the following figures.

Figure 3 depicts the total achievable rate against the number of BS antennas for three precoding schemes. In our simulations, we assume that the number of users is $K = 10$ and the input SNR is 5 dB. As we can see, the total achievable rate increases when the number of BS antennas grows, which implies that the large-scale antenna dramatically benefits the achievable sum rate. Furthermore, we observe that at the same configuration, the achievable rate with ZF and MMSE precoding schemes is more than double that with MRT scheme, and the total achievable rate with MMSE precoding scheme is always better than that with ZF precoding scheme, which implies that the MMSE precoding scheme is the best choice for massive multiuser MIMO system.

In Fig. 4, we depict the total achievable rate varies with the number of users for three precoding schemes. In simulations, the number of BS antennas is $N_t = 70$ and the input SNR is 5 dB, and the number of served user changes from 10 to 70. We can see that the total achievable

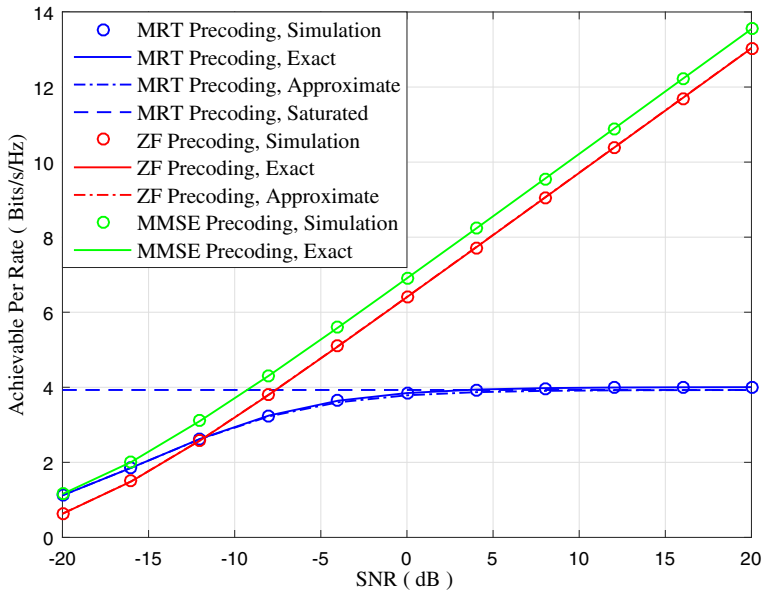

Fig. 2 Comparison of the achievable per rate of the *k*th user versus SNR for MRT, ZF, and MMSE precoding schemes. Results are shown for N_t= 128 and $K = 10$

rate grows with the number of users for MRT precoding schemes, since channel vector between users nearly tends to orthogonal and results in interference between users are eliminated. However, there is an optimal number of users that achieves the total achievable rate maximization for the ZF and MMSE precoding schemes. This is because when the number of users is small, increasing the number can effectively improve the spatial diversity and multiplexing gain ordered by the massive MIMO systems. The total achievable rate is increase rapidly. But when the numbers of users exceed the optimal value, the inter-user interference becomes dominant. Therefore, the total achievable rate for the massive MIMO systems declined gradually.

5 Conclusions

We quantized the downlink achievable ergodic rate in multiuser massive MIMO system, where the BS has the

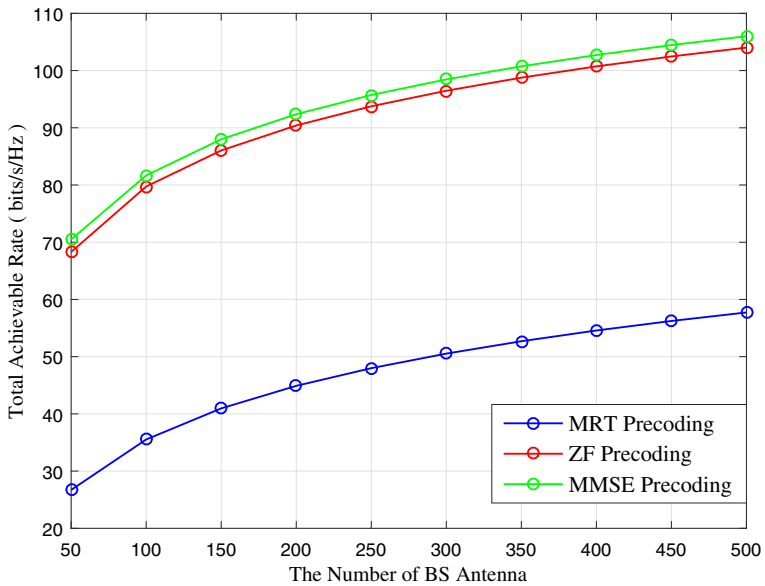

Fig. 3 Comparison of the total achievable rate versus the number of BS antennas for MRT, ZF, and MMSE precoding schemes. Results are shown for SNR $\rho = 5$ dB and $K = 10$

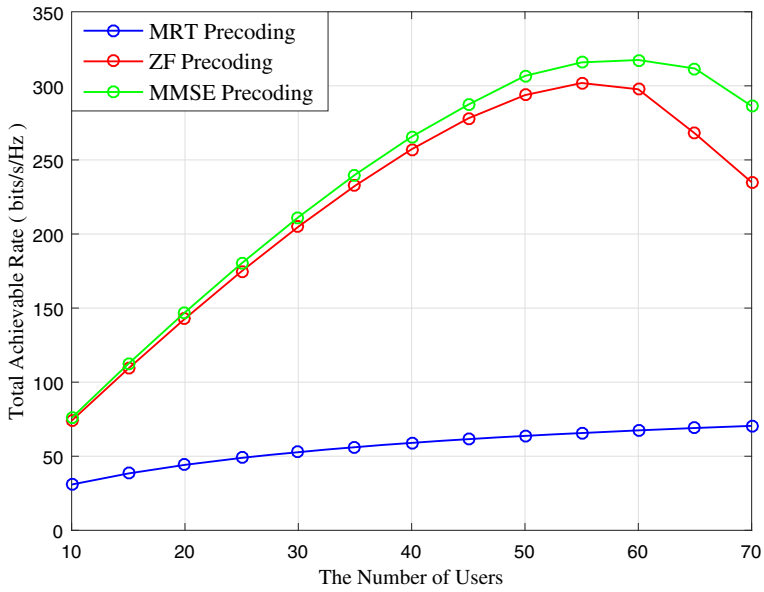

Fig. 4 Comparison of the total achievable rate versus the number of users for MRT, ZF, and MMSE precoding schemes. Results are shown for $N_t = 70$ and SNR $\rho = 5$ dB

ideal CSI and adopted the three types of different linear precoding schemes. The deterministic equivalent expressions of the achievable ergodic rate were obtained for the MRT, ZF, and MMSE precoding schemes. It is found that the ZF and MMSE precoding schemes achieve a higher achievable rate than MRT at the high SNR case. On the contrary, the achievable ergodic rate with MRT precoding scheme outperforms the ZF precoding schemes at the low SNR case. Moreover, for MRT precoding scheme, the achievable ergodic rates tend to converge to fixed constant when the input SNR goes without bounds. In addition, we also found that the total achievable rate does not increase with the number of users for the ZF and MMSE precoding schemes, which exists when the optimal number of users achieves the total achievable rate maximization. In the future, we attempt to extend our work in this paper with some other existing wireless techniques [43–45], which aim to improve the performance of massive MIMO system.

Endnotes

[1] The Rayleigh fading channel is the special case of the Ricean channel channel, but it is very different from the correlated fading channels. Thus, the detailed parameter set about the correlated fading channels can be found in the works [46–48].

[2] For simplicity, we use superscript $*$ replace the different precoding schemes, which shall be denotes the "MRT", "ZF" or "MMSE", respectively.

Appendix 1

To proceed with the proof, we recall the achievable ergodic rate of the user k in (4). Since the achievable ergodic rate per user is dependent to each other, by transforming the denominator to the numerator in internal term of log function, the achievable rate in (4) can be reformulated as

$$R_k^{\mathrm{MRT}} = \mathbb{E}\left\{\log_2\left(\frac{1+\rho\sum_{j=1}^{K}\left|\mathbf{h}_k^H\mathbf{w}_j\right|^2}{1+\rho\sum_{j=1,j\neq k}^{K}\left|\mathbf{h}_k^H\mathbf{w}_j\right|^2}\right)\right\}, \tag{33}$$

The expectation is taken over all fast fading coefficients; it is still challenging to directly give the p.d.f. of the SINR term. Herein, we further decompose it into two subexpressions (34), which can be found at the top of the next page.

$$\begin{aligned} R_k^{\mathrm{MRT}} = &\underbrace{\mathbb{E}\left\{\log_2\left(1+\rho\underbrace{\sum_{j=1}^{K}\left|\mathbf{h}_k^H\mathbf{w}_j\right|^2}_{X}\right)\right\}}_{I_1} \\ &\underbrace{-\mathbb{E}\left\{\log_2\left(1+\rho\underbrace{\sum_{j=1,j\neq k}^{K}\left|\mathbf{h}_k^H\mathbf{w}_j\right|^2}_{Y}\right)\right\}}_{I_2} \end{aligned} \tag{34}$$

To obtain the exact expression of $I_1$and I_2, we first need to attain the p.d.f.d of random variables X and Y, respectively. Since the entries of $\mathbf{h}_k$ are i.i.d. complex Gaussian random variables, according to (34), we can easily have the following distribution results

$$\left|\mathbf{h}_k^H \mathbf{w}_j\right|^2 = \begin{cases} \Gamma\left(N_t, 1\right), k = j \\ \Gamma\left(1, 1\right), k \neq j. \end{cases} \tag{35}$$

According to the above formulation, we observe that the K random variables $\left|\mathbf{h}_k^H \mathbf{w}_1\right|^2, \left|\mathbf{h}_k^H \mathbf{w}_2\right|^2, \ldots, \left|\mathbf{h}_k^H \mathbf{w}_K\right|^2$ follows Gamma distribution and are mutually independent. For the random variables $X = \sum_{j=1}^{K} \left|\mathbf{h}_k^H \mathbf{w}_j\right|^2$, it consists of a sum of K Gamma distribution, where each Gamma distribution has the different shape coefficient of N_t for $k = j$ case and one for the $j \neq k$ case, as well as the identical scale coefficient of 1. With the help of the results in [49], we know that $\rho = N_t + K - 1$, $\beta_1 = 1$ and $\delta_n = 1$. By substituting these results into (3) and while some basic manipulations, the p.d.f. of $X$is given by

$$f_X(x) = \frac{x^{N_t+K-2} e^{-x}}{\Gamma\left(N_t + K - 1\right)}. \tag{36}$$

Next, we further study the random variable $Y = \sum_{j=1, j\neq k}^{K} \left|\mathbf{h}_k^H \mathbf{w}_j\right|^2$ and see that is consists of a sum of K Gamma distribution, where each gamma distribution has the identical shape coefficient and scale coefficient, where the rate coefficient α is positive for all $j = 1, 2, \ldots, k-1, k+1, \ldots, K$ are identical. Using a similar approach as in [49, 50], the p.d.f. of $Y$is expressed as

$$f_Y(y) = \frac{x^{K-2} e^{-x}}{(K-2)!}. \tag{37}$$

Now, we have derived the p.d.f.s of the random variable X and Y, which can be offered in (36) and (37). Next, we will utilize the derived p.d.f.s and further evaluate the expressions of $I_1$and I_2, respectively, which can be rewritten as

$$I_1 = \log_2(e) \int_0^{\infty} \ln\left(1 + \rho X\right) f_X(x) dx \tag{38}$$

and

$$I_2 = \log_2(e) \int_0^{\infty} \log_2\left(1 + \rho Y\right) f_Y(y) dy. \tag{39}$$

To this end, although we have derived the p.d.f.s of random variances X and Y, respectively, the integral function in (38) and (39) is hard to calculate because it involves a special function. To solve this difficulty, we shall apply the integration identity, which is provided in [51] as follows:

$$\int_0^{\infty} \ln\left(1 + a\lambda\right) \lambda^{q-1} e^{-b\lambda} d\lambda = \left(q-1\right)! e^{b/a} b^{-q} \sum_{h=1}^{q} \mathrm{E}_h\left(\frac{b}{a}\right). \tag{40}$$

Consequently, $I_1$and I_2 can be calculated as

$$I_1 = \log_2(e) e^{\frac{1}{\rho}} \sum_{h=1}^{N_t+K-1} E_h\left(\frac{1}{\rho}\right) \tag{41}$$

and

$$I_2 = \log_2(e) e^{\frac{1}{\rho}} \sum_{h=1}^{K-1} E_h\left(\frac{1}{\rho}\right). \tag{42}$$

Substituting (41) and (42) into (34), and along with some basic manipulations, which completes the proof.

Appendix 2

As mentioned above, the elements of $\mathbf{H}$ are i.i.d. complex Gaussian random variances. According to the random matrix theory [52], the p.d.f. of γ_k is expressed as

$$p\left(\gamma_k\right) = \frac{e^{-\gamma_k}}{\left(N_t - K\right)!} \gamma_k^{N_t - K}. \tag{43}$$

According to (13), the expected is solved by calculating the following integral equivalent

$$R_k^{\mathrm{ZF}} = \log_2(e) \int_0^{\infty} \ln\left(1 + \rho\gamma_k\right) p\left(\gamma_k\right) d\gamma_k. \tag{44}$$

With the help of the p.d.f. of γ_k, we substitute this result into (44) while utilizing the integration identity provided in (40), and we finish the proof.

Appendix 3

Since we consider the massive MIMO system under Rayleigh fading channel model, the entries of $\mathbf{H}$ are i.i.d. complex Gaussian random variances, and it is analytically intractable to derive the exact p.d.f. of z_k. To proceed, we would like to directly use the result in [42], which provides an approximate expression on the p.d.f. of z_k. By applying the result in ([42], Eq.35), the p.d.f. of z_k can be expressed as

$$p\left(z_k\right) = \frac{{z_k}^{\alpha-1} e^{-z_k/\beta}}{\Gamma\left(\alpha\right) \beta^{\alpha}}. \tag{45}$$

Adopting the similar procedures in (44), the evaluation of R_k^{MMSE}can be given by

$$R_k^{\mathrm{MMSE}} = \log_2(e) \int_0^{\infty} \ln\left(1 + z_k\right) p\left(z_k\right) dz_k. \tag{46}$$

where $z_k$has been shown in (27), By substituting (45) into (46) and utilizing the integration identity [53]

$$\int_0^{\infty} \ln\left(\lambda\right) e^{-b\lambda} d\lambda = -\frac{1}{b}\left(e + \ln b\right). \tag{47}$$

We derive the exact expression as (5) after some mathematical manipulations, which completes the proof.

Abbreviations
5G: Fifth generation; AWGN: Additive white Gaussian noise; BS: Base station; CSI: Channel state information; DPC: Dirty paper coding; FDD: Frequency division duplex; MIMO: Multiple-input multiple-output; MMSE: Minimum mean squared error; MRT: Maximum ratio transmission; QoS: Quality of service; TDD: Time division duplex; SNR: Signal-to-noise ratio; VP: Vector perturbation; ZF: Zero-forcing

Funding
This work was supported in part by the National Natural Science Foundation of China under Grants 61801132 and 61871139, the Natural Science Foundation of Guangdong Province under Grant 2018A030310338, the Project of Educational Commission of Guangdong Province of China under Grant 2017KQNCX155, the Innovation Team Project of Guangdong Province University under Grant 2016KCXTD017, the Guangdong Natural Science Funds for Distinguished Young Scholar under Grant 2014A030306027, the Science and Technology Program of Guangzhou under Grant 201807010103, and the Project of Hunan Provincial Department of Education under Grant 16A174.

Availability of data and materials
Mostly, I got the writing material from different journals as presented in the references. A MATLAB tool has been used to simulate my concept.

Authors' contributions
WT designed the idea and performed the experiments. WH and ZS have processed the data and written the manuscript. XY and LF gave valuable suggestions on the structuring of the paper and assisted in the revising and proofreading. All authors read and agreed the manuscript.

Competing interests
The authors declare that they have no competing interests.

Publisher's Note

Author details
[1]School of Computer Science and Educational Software, Guangzhou University, 510006 Guangzhou, People's Republic of China. [2]National Mobile Communications Research Laboratory, Southeast University, 210096 Nanjing, People's Republic of China. [3]College of Information Science and Engineering, Jishou University, 416000 Jishou, People's Republic of China. [4]School of Electrical and Information Engineering and the Institute of Physical Internet, Jinan University, 519000 Zhuhai, People's Republic of China.

Received: 22 April 2018 Accepted: 2 August 2018
Published online: 22 August 2018

References
1. K. Zheng, L. Zhao, J. Mei, B. Shao, W. Xiang, L. Hanzo, Survey of large-scale MIMO systems. IEEE Commun. Surveys Tuts. **17**(3), 1738–1760 (2015)
2. L. Lu, G. Y. Li, A.L. Swindlehurst, A. Ashikhmin, R Zhang, An overview of massive MIMO: Benefits and challenges. IEEE J. of Sel. Topics in Signal Processing. **14**(15), 136–146 (2014)
3. Y. Fang, G. Han, P. Chen, F.C.M. Lau, G. Chen, L. Wang, A survey on DCSK-based communication systems and their application to UWB scenarios. IEEE Commun. Surveys Tuts. **18**(3), 1804–1837 (2016)
4. C. Li, K. Song, D. Wang, F. Zheng, L. Yang, Optimal remote radio head selection for cloud radio access networks. Sci. China Inf. Sci. **59**, 10 (2016)
5. M. Zhang, W. Tan, J. Gao, S. Jin, Spectral efficiency and power allocation for mixed-ADC massive MIMO system. China Commun. **15**(3), 112–127 (2018)
6. X. Wang, H. Zhang, L. Fan, Y. Li, Performance of distributed switch-and-stay combining for cognitive relay networks with primary transceiver. Wirel. Personal Commun. **97**(2), 3031–3042 (2017)
7. M. Zhao, D. Deng, W. Zhou, L. Fan, Non-renewable energy efficiency optimization in energy harvesting relay-assisted system. Phys. Commun. **28**, 1–10 (2018)
8. F. Boccardi, R.W. Heath, A. Lozano, T.L. Marzetta, P. Popovski, Five disruptive technology directions for 5G. IEEE Commun. Mag. **52**(2), 74–80 (2014)
9. D.D. Nguyen, Y. Liu, Q. Chen, On the energy efficient multi-pair two-way massive MIMO af relaying with imperfect CSI and optimal power allocation. IEEE Access. **6**, 2589–2603 (2018)
10. G. Pan, H. Lei, Y. Deng, L. Fan, J. Yang, Y. Chen, Z. Ding, On secrecy performance of MISO SWIPT systems with TAS and imperfect CSI. IEEE Trans. Commun. **64**(9), 3831–3843 (2016)
11. J. Yuan, S. Jin, W. Xu, W. Tan, M. Matthaiou, K.K. Wong, User-centric networking for dense C-RANS: High-SNR capacity analysis and antenna selection. IEEE Trans. Commun. **65**(11), 5067–5080 (2017)
12. S. Payami, F. Tufvesson, Channel measurements and analysis for very large array systems at 2.6 GHz. Proc. Eur. Conf. Antennas Propag, 15–21 (2012)
13. X. Gao, O. Edfors, F. Rusek, F. Tufvesson, Linear pre-coding performance in measured very-large MIMO channels. Proc. IEEE VTC, 35–40 (2011)
14. B. Liu, Q. Zhu, W. Tan, H. Zhu, Congestion-optimal WIFI offloading with user mobility management in smart communications. Wirel. Commun. Mob. Comput, 1–15 (2018)
15. J. Hoydis, C. Hoek, T. Wild, S.T. Brink, Channel measurements for large antenna arrays. IEEE ISWCS., 264–273 (2012)
16. X. Lai, J. Xia, M. Tang, H. Zhang, J. Zhao, Cache-aided multiuser cognitive relay networks with outdated channel state information. IEEE Access. **6**, 21879–21887 (2018)
17. F. Zhou, L. Fan, X. Lei, G. Luo, H. Zhang, J. Zhao, Edge caching with transmission schedule for multiuser multirelay networks. IEEE Commun. Lett. **22**(4), 776–779 (2018)
18. F. Shi, L. Fan, X. Liu, Z. Na, Y. Liu, Probabilistic caching placement in the presence of multiple eavesdroppers. Wirel. Commun. Mob. Comput., 2104162 (2018). https://doi.org/10.1155/2018/2104162)
19. H. Yin, D. Gesbert, M. Filippou, Y. Liu, A coordinated approach to channel estimation in large-scale multiple-antenna systems. IEEE J. Sel. Areas Commun. **31**(2), 264–273 (2013)
20. S. Jin, X.Y. Wang, Z. Li, K.K. Wong, Zero forcing beamforming in massive MIMO systems with time-shifted pilots. Proc. IEEE ICC, 4108–4114 (2014)
21. A. Ashikhmin, T. Marzetta, Pilot contamination precoding in multicell large scale antenna systems. Proc. IEEE ISIT, 1137–1141 (2012)
22. C. Li, S. Zhang, P. Liu, F. Sun, J.M. Cioffi, L. Yang, Overhearing protocol design exploiting inter-cell interference in cooperative green networks. IEEE Trans. Veh. Technol. **65**(1), 441–446 (2016)
23. J. Li, M. Wen, X. Jiang, W. Duan, Space-time multiple-mode orthogonal frequency division multiplexing with index modulation. IEEE Access. **5**, 23212–23222 (2017)
24. W. Tan, S. Jin, C.K. Wen, J. Tao, Spectral efficiency of multi-user millimeter wave systems under single path with uniform rectangular arrays. EURASIP J. Wirel. Commun. Netw. **181**, 458–472 (2017)
25. E. Bjornson, L. Sanguinetti, J. Hoydis, M. Debbah, Optimal Design of Energy-Efficient Multi-User MIMO Systems: Is Massive MIMO the Answer. IEEE Trans. Wirel. Commun. **14**(6), 3059–3075 (2015)
26. C. Li, K. Song, Y. Li, L. Yang, Energy efficient design for multiuser downlink energy and uplink information transfer in 5G. Sci. China Inf. Sci. **599**(2), 30–48 (2016)
27. H.Q. Ngo, E.G. Larsson, T.L. Marzetta, Energy and spectral efficiency of very large multiuser MIMO systems. IEEE Trans. Commun. **61**(4), 1436–1449 (2013)
28. Q. Zhang, S. Jin, K.K. Wong, H.B. Zhu, Power scaling of uplink massive MIMO systems with arbitrary-rank channel means. IEEE J. Sel. Top. Signal. Process. **57**(3), 841–849 (2014)
29. H. Yang, T.L. Marzetta, Performance of conjugate and zero-forcing beamforming in large-scale antenna systems. IEEE J. Sel. Areas Commun. **31**(2), 172–179 (2013)
30. Y.G. Lim, C.B. Chae, G. Caire, Performance analysis of massive MIMO for cell-boundary users. IEEE Commun. Mag. **19**(9), 341–355 (2013)
31. W. Tan, G. Xu, E.D. Carvalho, L. Fan, C. Li, Low cost and high efficiency hybrid architecture massive MIMO systems based on DFT processing. Wirel. Commun. Mob. Comput. **2018**, 1–13 (2018)
32. D. Deng, M. Yu, J. Xia, Z. Na, J. Zhao, Q. Yang, Wireless powered cooperative communications with direct links over correlated channels. Phys. Commun. **28**, 147–153 (2018)
33. M. Abramowitz, *IA Stegun.Handbook of Mathematical Functions*. (Dover, New York, 1974)
34. T.L. Marzetta, Noncooperative cellular wireless with unlimited numbers of base station antennas. IEEE Trans. Wirel. Commun. **9**(11), 3590–3600 (2010)

35. M. Costa, Writing on dirty paper. IEEE Trans. Inf. Theory. **29**(3), 439–441 (1983)
36. W. Tan, M. Matthaiou, S. Jin, X. Li, Spectral efficiency of DFT based processing hybrid architectures in massive MIMO. IEEE Wirel. Commun. Lett. **6**(5), 586–589 (2017)
37. X. Liu, X. Zhang, M. Jia, et al, 5G-based green broadband communication system design with simultaneous wireless information and power transfer. Phys. Commun. **28**, 130–137 (2018)
38. R.M. Corless, G. Gonnet, G. Hare, D. Jeffrey, D. Knuth, On the lambert W function. Advances in Computational Mathem. **5**(4), 329–359 (1996)
39. J. Yang, H. Wu, M. Wang, Y. Liang, Prediction and optimization of radiative thermal properties of nano TiO2 assembled fibrous insulations. Int. J. Heat Mass Trans. **117**, 729–739 (2018)
40. J. Yang, H. Wu, M. Wang, S. He, H. Huang, Prediction and optimization of radiative thermal properties of ultrafine fibrous insulations. Appl. Therm. Eng. **104**, 394–402 (2016)
41. Y. Liang, H. Wu, G. Huang, J. Yang, H. Wang, Thermal performance and service life of vacuum insulation panels with aerogel composite cores. Energy Build. **154**, 606–617 (2017)
42. P. Li, D. Paul, R. Narasimhan, J. Cioffi, On the distribution of SINR for the MMSE MIMO receiver and performance analysis. IEEE Trans. Inf. Theory. **52**(1), 271–286 (2006)
43. N. Zhao, F.R. Yu, V.C.M. Leung, Opportunistic communications in interference alignment networks with wireless power transfer. IEEE Trans. Wirel. Commun. **22**(1), 88–95 (2015)
44. N. Zhao, Y. Cao, F.R. Yu, Y. Chen, M. Jin, V.C. Leung, Artificial noise assisted secure interference networks with wireless power transfer. IEEE Trans. Veh. Technol. **67**(2), 1087–1098 (2018)
45. Y. Cao, N Zhao, F. Yu, M. Jin, Y. Chen, J. Tang, V.M Leung, Optimization or alignment: Secure primary transmission assisted by secondary networks. IEEE J. Sel. Areas Commun. **36**(4), 905–917 (2018)
46. L. Fan, R. Zhao, F. Gong, N. Yang, G.K. Karagiannidis, Secure multiple amplify-and-forward relaying over correlated fading channels. IEEE Trans. Commun. **65**(7), 2811–2820 (2017)
47. J. Xia, F. Zhou, X. Lai, *et al*, Cache aided decode-and-forward relaying networks: From the spatial view. Wirel. Commun. Mob. Comput. **2018**(Article ID: 5963584), 1–13 (2018)
48. R. Zhao, Y. Yuan, L. Fan, Y. He, Secrecy performance analysis of cognitive decode-and-forward relay networks in Nakagami-m fading channels. IEEE Trans. Commun. **65**(2), 549–563 (2017)
49. P.G. Moschopoulos, Distribution of the Sum of Independent Gamma Random Variables. Ann. Inst. Statist. Math. **37**(2), 541–544 (1985)
50. J. Yang, H. Wu, G. Huang, Y. Liang, Y. Liao, Modeling and coupling effect evaluation of thermal conductivity of ternary opacifier/fiber/aerogel composites for super-thermal insulation. Mater. Des. **133** (5), 224–236 (2017)
51. G. Alfano, A. Lozano, A.M. Tulino, Verdú S., Mutual information and eigenvalue distribution of MIMO Ricean channels. Proc. IEEE ISIT, 10–13 (2004)
52. A. Grant, Rayleigh fading multi-antenna channels. EURASIP J. Appl. Signal Process. **2002**(3), 316–329 (2002)
53. I.S. Gradshteyn, I. M. Ryzhik, *Table of Integrals, Series, and Products, 7th edition*. (Academic Press, San Diego, 2007)